Testing a Flexible Configuration of a Solar-Assisted Heat Pump with PVT Collectors for Domestic Hot Water Production

George Meramveliotakis[1,2], George Kosmadakis[1], Marika Pilou[1] and Sotirios Karellas[2]

[1] Thermal Hydraulics and Multiphase Flow Laboratory, National Centre for Scientific Research "Demokritos", Agia Paraskevi (Greece)

[2] Laboratory of Steam Boilers and Thermal Plants, Zografou, School of Mechanical Engineering, National Technical University of Athens, 9 Heroon Polytechniou St., Zografou Campus, 15780 Athens, (Greece)

Abstract

A solar energy based pilot system located in Athens, Greece, is examined experimentally for covering hot water demand. The system consists of a heat pump with vapor injection coupled with low concentrating stationary PVT collectors in a flexible configuration. The produced heat of the collectors is delivered to the hot water tank directly covering the demand with the heat pump operating as an air-source unit and supporting the charging when its temperature gets below 45 ^{o}C. This work examines the performance and the capacity of the system with two different draw-off profiles (medium and large) based on EU standard EN16147:2017 simulated by an electronic valve with a constant water mass flow rate and a pre-defined time schedule during the day. Tests have been conducted for both profiles during summer days with the aim to evaluate the system performance in terms of heat balances and net electricity consumption once considering the power production of the PVT collectors as well.

Keywords: Heat pump, PVT collector, residential building, domestic hot water, tapping profile

1. Introduction

The total required energy for space heating (SH) and domestic hot water (DHW) is estimated to more than 20% of the entire energy demand in EU28 buildings (Bertoldi et al., 2018). According to Pezzuto et al. (Pezzutto et al., 2019), over 85% of the total energy (about 3315 TWh/y) is provided for space heating while about 600 TWh/y is used for DHW needs. Also, 84% of the total energy demand for space heating and DHW production is covered by fossil fuels (e.g. gas boilers) while only 16% from renewable energy sources (Galindo Marina et al., 2016). At the same time, the European council has set 4 key milestones within the 2030 framework for climate and energy including a 40% cut in greenhouse gas (GHG) emissions compared to 1990 levels, such as at least a 32% share of renewables (Bertoldi et al., 2018). As a result, the adoption of renewable energy solutions in the building sector is getting more than crucial in order these targets to be achieved.

Several regulations and policies that have been into force have led to the decrease of space heating demand through actions such as building insulation and energy management advancements. On the other hand, the domestic hot water demand remains about the same (Guo and Goumba, 2018). Additionally, the DHW preparation is something strongly behavioral related to the occupants that requires consideration of both the energy system and the draw-off profile, which affects the energy consumption and consequently the performance and efficiency of the systems (Zhou et al., 2022). Thus, the relevant objective is formed to introduce higher efficiency systems combining also renewable energy sources and to consider the effect of draw-off profile variation to the system operation.

The use of solar energy is one of the most promising renewable energy sources to meet the needs for heating and DHW with wide use. The benefits are mainly related to the significant reduction of operational costs especially during mid-seasons and summer due to the adequate amounts of solar irradiation which eliminates the operation of typical boilers during those periods (Tian et al., 2019). On the other hand, solar collectors can only provide hot water when irradiation is sufficient emerging the need of integrating thermal storage and auxiliary systems in order to ensure that heat is delivered when needed. A promising auxiliary heating system is a heat pump whose use is increasing because it combines high efficiency, flexibility in integration with renewables, and reduced final energy consumption, especially when it is supplied with low temperature heat instead of ambient air (Pilou et al., 2021). Additionally, many efforts are on-going to decrease the carbon footprint of heat pump systems especially by employing new low global warming potential (GWP) refrigerants such as natural refrigerants like carbon dioxide

Selection and/or peer review under responsibility of Scientific Committee
doi:10.18086/eurosun.2022.08.07 Available at http://proceedings.ises.org

(R744), propane (R290), and new generation hydrofluoroolefins (HFOs) (Meramveliotakis et al., 2022, 2021).

Air-source heat pumps for DHW production have a large potential and much research has been done to explore it. The main interest focuses on methods to enhance the system performance (expressed through the coefficient of performance – COP) and capacity, with vapor injection technique (Li et al., 2022) introducing significant improvements, especially in cold climates. At the same time, decreasing the GWP of the heat pump system is a crucial objective and for that natural refrigerants such as CO_2 or CO_2/Ammonia (Ju et al., 2018) blends are examined.

A more efficient alternative is the solar-assisted heat pump (SAHP) which combines solar thermal collectors and a heat pump in a single configuration to meet DHW demand (Sun et al., 2015). The operation and performance of SAHP systems have been studied both numerically (Sterling and Collins, 2012) and experimentally (Panaras et al., 2014) resulting to significant energy savings compared to fired heaters (Panaras et al., 2013). Another study (Long et al., 2021) investigated a hybrid solar hot water and air source heat pump flexible system allowing in series, parallel and preheating type connection of solar water for hot water heating. The results showed that the external conditions (ambient temperature and solar irradiation) play an important role in the overall performance and the combined heating system showed 8.4%, 7.1% and 15.8% better seasonal performance compared to the parallel, in series and preheating systems as single units.

By further advancing the SAHP configuration, the solar collectors can be replaced by hybrid photovoltaic thermal (PVT) collectors that produce both heat and electricity (Lämmle et al., 2017). This concept increases the solar energy utilization compared to separate PV and solar thermal systems (Vaishak and Bhale, 2019). Pilou et al. (Pilou et al., 2022) investigated numerically the integration of PVT collectors, multi-source heat pump and ground heat exchanger in office buildings for cold (Copenhagen) and hot (Athens) climates pointing out a high COP of the heat pump (about 4.2 for winter in Athens and 3.8 for winter in Copenhagen) with also high share of renewables reaching values over 75% for Athens and 50% for Copenhagen.

Based on the above, a coupling of a dual-source heat pump (air or water) with PVT collectors as part of a pilot system located in Athens, Greece, is examined. The system design allows exploiting all the produced PVT heat by either directly charging the DHW tank or charging a separate tank at a low temperature which acts as the heat source to the heat pump, for increasing its COP (Buker and Riffat, 2016). In this study, the performance of the air-source only system is investigated experimentally with the high temperature heat production of the PVT charging a tank to cover hot water demand whereas the heat pump is the auxiliary system to support the heat production. The system is tested under two taping water profiles according to the EN16147:2017 standard for water-heaters, corresponding to the "M" (Medium) and "L" (Large) profile of the standard.

2. System description

2.1. Experimental Setup

The experimental setup consists of a solar assisted heat pump with a heating capacity of 15 kW initially designed for heating, cooling and DHW production. The main system components are highlighted in Fig. 1 including the PVT collectors for producing heat and electricity and the heat pump providing either cooling or heating via reversing its thermodynamic cycle with the use of 4-way valves.

(a) (b)

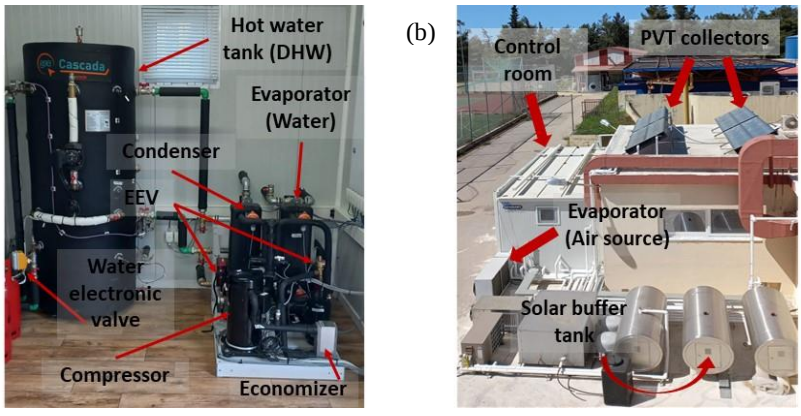

Fig. 1: The main components of the experimental setup. (a) Heat pump and DHW tank inside the control room, (b) Outdoor installation highlighting the PVT collectors, air source evaporator and auxiliary units

The schematic diagram of the complete experimental setup is shown in Fig. 2, with the main interest focused on

DHW production, while the system components which are not in operation are illustrated with gray transparent color (mainly the solar buffer tank that is charged by the collectors and enables the solar-assisted heat pump operation). The heat pump is working only with ambient air as heat source (evaporator side) while the hot side (condenser) is delivering the produced heat to the DHW tank through a closed loop water circuit. Additionally, the same tank is connected with 4 PVT collectors installed in series by two, achieving a parallel integration between solar circuit and heat pump.

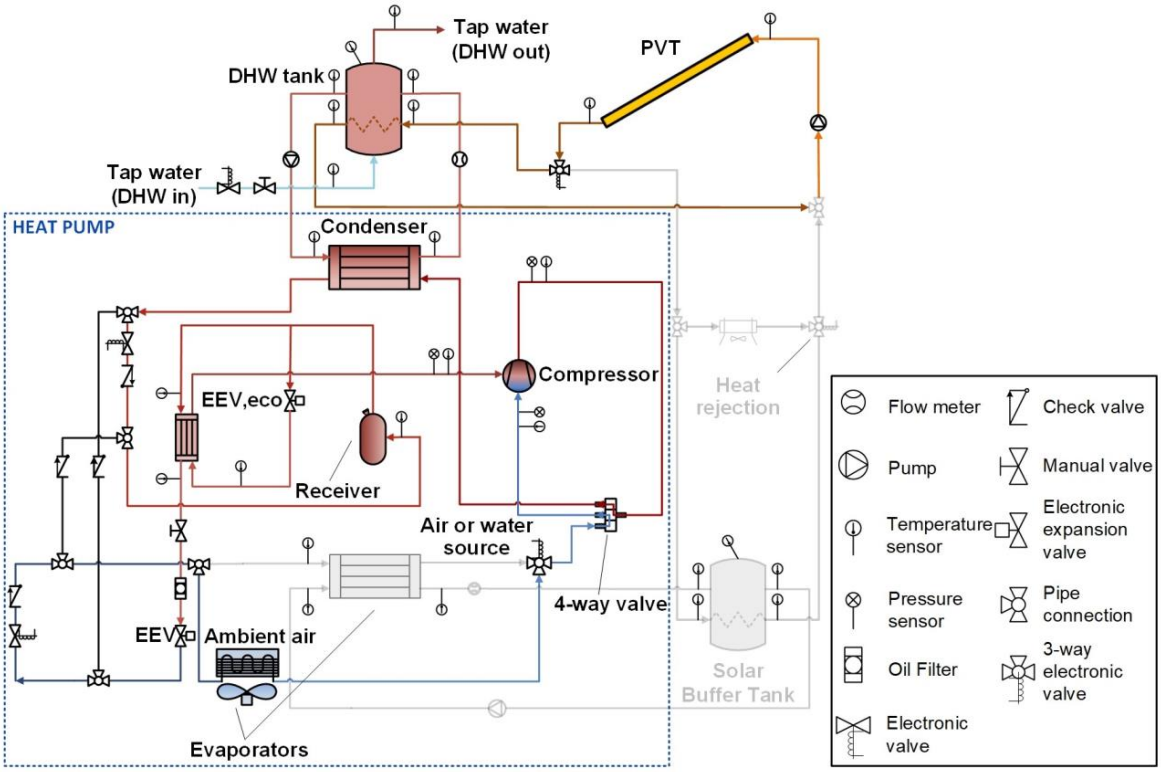

Fig. 2: Schematic diagram of the solar assisted heat pump integrated with the DHW water tank

2.2. Heat pump

The heat pump is equipped with a Copeland ZH13KVE scroll compressor initially provided for R407C with 11.7 m^3/h displacement at 50 Hz. The compressor is intended for heating applications equipped with an economizer port to allow vapor injection operation. The refrigerant is the HFO blend R454C with a low GWP of 148, zero ozone depletion potential (ODP) and was selected due to its similar properties to R407C and its performance was initially assessed with the use of a validated heat pump model in EES software (Kosmadakis et al., 2020). The total charge is 5 kg of refrigerant and a receiver with a volume of 1.5 lt has been placed after the condenser to account for changes in the operating conditions. All three plate heat exchangers (HEX) (Fig. 2) are manufactured by SWEP with some over-surfacing to ensure the performance of the heat exchanger is kept at desirable levels even during dynamic operation. Also, a custom-made fin and tube air heat exchanger is included, with 55.47 m^2 total exchange surface and capacity of 21.77 kW. The selection of either air or water source evaporator is attained by adjusting the flow direction of an electronic 3-way valve installed at the refrigerant circuit, and thus generating two different options for the working fluid accordingly. In this work, this valve always directs the refrigerant flow through the air source evaporator.

In the heat pump configuration, a vapor injection circuit (VI) is also implemented to enhance its performance and increase the system's capacity (Kwon et al., 2017; Tello-Oquendo et al., 2019). The injection mass flow rate is adjusted by an electronic expansion valve placed at the economizer line, with a fixed superheat of 7 K. A part of the main flow is expanded to an intermediate pressure and then directed to the economizer to be evaporated by the liquid flow. The vapour then enters the compressor and is mixed with the compressed vapour, resulting to a lower superheat of the mixture. The main liquid flow of the refrigerant passes through the main electronic expansion valve also with a fixed superheat of 7 K and then enters the air source evaporator and finally to the compressor suction, closing the cycle. Tab. 1 shows the main components of the heat pump.

Tab. 1: Main components of the heat pump

Component	Type	Description
Copeland ZH13KVE	Scroll compressor with VI port	11.70 m^3/h displacement at 50 Hz
SWEP B80Hx30/1P	Plate heat exchanger	30 plates with 1.68 m^2 of total heat transfer area for both evaporator and condenser
SWEP B5THx34/1P	Plate heat exchanger	34 plates with 0.384 m^2 of total heat transfer area for the economizer
Danfoss T2/TE2 134	Electronic expansion valve	Expansion valve for vapor injection circuit with 7 K adjusted superheat
Parker Sporlan ODF ST SEI-1-10-S	Electronic expansion valve	Main expansion valve with 7 K adjusted superheat
Custom made air fan coil	Fin and tube heat exchanger	4 circuits, with 3 rows (16 tubes/row) with a total surface of 55.47 m^2
OCS, type RV1CC130X250	Refrigerant receiver	Volume of 3.0 lt, design pressure 32 bar
RANCO, V10-314120200	4-way valve	Nominal capacity of 35 kW, for switching heating and cooling mode
Castel 6690M/7A6	3-way valve	For switching water and air source evaporator

2.3. PVT collectors

The PVT collector of the pilot system includes a low-concentration (concentration factor 1.5) stationary parabolic reflector with an improved design for increasing the incidence angle modifiers (IAMs) over a large range of incident angles. The solar irradiation is concentrated onto an aluminium absorber that carries on both upper and bottom side PV cells laminated with a highly transparent and electrically insulating silicone. The upper side operates exactly as a standard PV module, while the bottom side receives the concentrated solar radiation from the reflector. Also, a glazed protection is installed and the supporting housing of the collector is made of plastic and metal compounds. The cooling medium in the PVT solar circuit is a water/glycol (Tyfocor L) mixture with 40% by volume concentration of glycol, including also anticorrosive additives to protect the aluminium receiver. The produced heat is delivered through stainless steel piping to the DHW tank with an immersed heat exchanger with a total surface of 1.7 m^2. The total area of each PVT collector is 2.31 x 0.955 m (2.15 m^2) and its thermal and electrical capacity is 1250 and 250 W respectively at standard conditions. The experimental setup consists of 4 collectors placed with 31^o tilt and south orientation (zero azimuth angle), connected in series by two (due to the expected pressure drop in each collector) creating two parallel loops. The flow rate of each loop is calculated with the use of a typical specific flow rate of 0.02 lt/m^2s, resulting to about 155 lt/h per loop and 310 lt/h in total. Furthermore, as depicted in Fig. 1, the solar circuit is equipped with a Wilo circulating pump, type Para 25-130/7-50, and a heat rejection dry cooler system with a capacity of 5 kW to protect the collectors from over-heating.

2.4. Domestic hot water tank

The experimental setup includes a 300 liters capacity water tank for domestic hot water preparation. The tap water is heated and then discharged (open type). A controllable valve is placed at the water inlet with an on-off functionality based on a tapping profile. Temperature sensors are installed at the inlet and outlet of the tank to measure the cold and hot water temperatures as well as a flow rate meter. In addition, temperature sensors are placed in available slots at different heights of the tank. The PVT collectors charge the bottom part, while the heat pump the upper one. This results to a strong stratification and therefore this tank is placed vertically as it is shown in Fig. 2. The DHW tank includes two immersed heat exchangers (spiral coils) made of stainless steel 316L, one for the solar circuit and another for the tap water. Furthermore, the design of the tank includes also a Grundfos water pump to recirculate the tap water and achieve the defined supply temperature for domestic hot water, which is defined at 45 ^{o}C at all times.

2.5. Measuring instruments and their accuracy

Various sensors are installed for measuring temperatures, pressures and flow rates at different positions of the pilot system. All the measurements are collected every one minute by a PLC unit which acts both as control device of the

heat pump and as a data logger by implementing additional analog to digital communication cards with analog inputs from various sensors. The selected PLC is the Mitsubishi FX5U-32MR-ES with 16 digital inputs and 16 digital outputs and two integrated channels with analog input and 1 analog output. Concerning the heat pump configuration, there are 3 pressure and 12 temperature sensors (8 for the refrigerant and 4 for the water lines). The power consumption of the heat pump (three-phase) and the power production of the collectors (single-phase, AC side) is recorded by two power meters. Additionally, two pyranometers are used to measure total and diffuse solar irradiation in order to provide a direct evaluation of the PVT collectors performance. With the use of the above sensors it is possible to process the measured data and calculate the thermal flows of all components, the electricity consumption and production as well as performance and efficiency indicators. The list of sensors is given in Tab. 2, providing their type, accuracy and measured property.

Tab. 2: List of sensors in the pilot system with their accuracy

Property	Sensor type	Accuracy	Quantity	Description
Temperature	Pt100 3-wire, with transducer (4-20 mA)	<0.1 K	18	Temperature of water, brine and refrigerant calibrated in the range of 0-100 ^{o}C for water and -20 – +80 ^{o}C for refrigerant
Temperature	NTC, 2-wire	0.1 K	2	Temperatures of the refrigerant at the outlet of evaporator and economizer for superheat control
Outdoor temperature	Pt100, 4-wire with radiation shield	<0.4 K	1	Outdoor temperature for evaluating PVT collector performance and air-source operation of the heat pump
Pressure	Pressure transmitter ESCP-MIT1	0.25% of FS	3	0-10 bar for the evaporator and economizer lines, 0-30 bar for the condenser line
Flow rate	Electromagnetic flow rate meter with ModBus	<0.5% of measured value	4	Flow rate of DHW profile, solar brine and water flow in the evaporator and condenser
Electricity	Power meter with current transformers and ModBus	<0.2% of measured value	2	Electricity consumption of the heat pump and all auxiliaries. Electricity production of the PVT collectors (total).
Total solar irradiation	Pyranometer with ModBus	<5 W/m^2	1	Total solar radiation on the collector's surface (mounted on one collector with the same tilt and azimuth)
Diffuse solar irradiation	Pyranometer with shadow ring with analog signal 0-20 mV	<10 Wm^2	1	Diffuse radiation with shadow ring blocking the direct irradiation to the sensor

3. Experimental Design and performance calculations

3.1. Experimental procedure and DHW profiles

The experimental procedure is structured in a way to examine the performance of the pilot system in terms of DHW production. For that reason, the sub-system that includes the heat pump (air-source operation) – PVT collectors – DHW tank was evaluated under two test series performed using two different taping profiles (different daily loads) in two consecutive summer days (30 and 31 of July 2022) at the facilities of the National Center of Scientific Research "Demokritos" in Athens, Greece. Each experiment lasted for 24 hours in order to obtain the daily behavior of the system. Also, prior to the experimental procedure, the system has been operated for at least 2 days in order to minimize temperature fluctuations aiming to initialize the measuring conditions exactly as a typical operational day and to avoid taking into account fewer or more thermal loads. The DHW profile is pre-defined according to the

EN16147:2017 standard for water heaters, hot water storage appliances, and water heating systems ("Directive 2009/125/EC"). This standard defines a 24-h tapping cycle with a draw temperature and variable flow rate leading to the calculation of a total thermal energy demand per day. Taking into consideration the monthly average tap water temperature, the average daily thermal energy demand has a seasonal variation during the months with higher values in the winter (lower tap water temperature) and lower values in the spring and summer. According to this standard, the "M" (Medium profile – Day 1) and "L" (Large profile – Day 2) profiles have been selected and the average daily demand has been calculated as 4.68 kWh for "M" and 9.34 kWh for "L" profile during July. In order to integrate the two DHW profiles into the system operation, the hourly based DHW demand in kWh needs to be converted into an integral number which represents the opening time in minutes of an on-off electronic valve (constant water flow rate) placed at the inlet piping of DHW flow (Fig. 1). As a result, the two tapping profiles have been converted into valve opening time profiles with a flow rate of 0.355 m^3/h estimated with a best-fit procedure in order to achieve very close agreement with the standard's defined profiles. Both the tapping profiles of the standard and the time-dependent profiles of the electronic valve are depicted in Fig. 3.

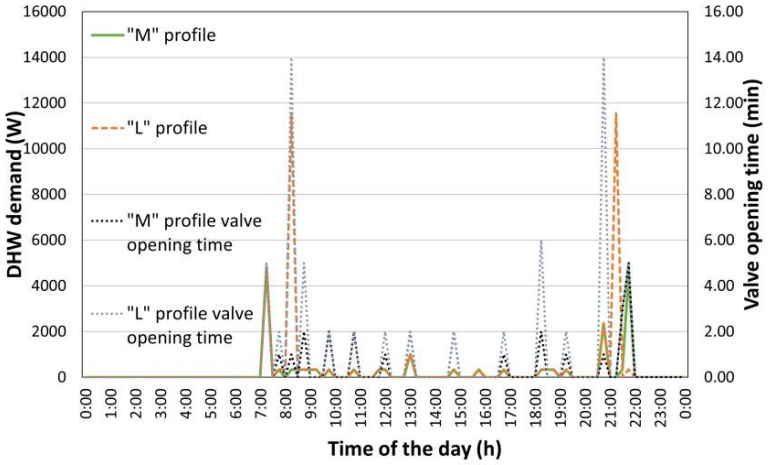

Fig. 3: DHW demand with "M" and "L" profiles of the EN16147:2017 standard and converted electronic valve opening profiles

3.2. Performance calculations

In this section, the basic performance indicators are presented. Concerning the heat pump evaluation, its capacity $\dot{Q}_{cond}$ is identified from the measured data (Eq. 1) while the system's COP is calculated with Eq. 2.

$$\dot{Q}_{cond}=\dot{m}_{w,cond}\cdot c_{p_{w,cond}}\cdot\left(T_{w,cond,out}-T_{w,cond,in}\right) \quad \text{(eq. 1)}$$

$$COP=\frac{\dot{Q}_{cond}}{P_{elec,tot}} \quad \text{(eq. 2)}$$

$\dot{m}_{w,cond}$ (kg/s) is the water mass flow at the condenser calculated from water flow measurements, c_p (kJ/kg·K) is the heat capacity at constant pressure and T (K) the temperature at specific conditions.

Regarding the PVT collectors, the heat production is identified via Eq. 3 while the produced electricity (P_{PVT}) is directly measured by the power meter. The collector's thermal and electrical efficiency is determined by Eqs. 4 and 5 while the total heat and electrical production is estimated by integrating the 1 – minute values over the whole day operation.

$$\dot{Q}_{th,PVT}=\dot{m}_{br,PVT}\cdot c_{p_{br,PVT}}\cdot\left(T_{br,PVT,out}-T_{br,PVT,in}\right) \quad \text{(eq. 3)}$$

$$n_{th,PVT}=\frac{\dot{Q}_{th,PVT}}{I_{t,total}*A_{col,tot}} \quad \text{(eq. 4)}$$

$$n_{el,PVT}=\frac{P_{PVT}}{I_{t,total}*A_{col,tot}} \quad \text{(eq. 5)}$$

where $I_{t,total}$ (kW/m^2) is the total solar irradiation on the titled collector surface and $A_{col,tot}$ the total surface of the 4 PVT collectors.

For DHW tank calculations, the heating load $\dot{Q}_{w,DHW}$ is determined by Eq. 6, while the total daily need for domestic hot water $Q_{w,DHW}$ in kWh is calculated by the integral of Eq. 7.

$$\dot{Q}_{w,DHW}=\dot{m}_{w,DHW}\cdot c_{p_{w,DHW}}\cdot\left(T_{w,DHW,out}-T_{w,DHW,in}\right) \quad \text{(eq. 6)}$$

$$Q_{w,DHW}=\frac{\int \dot{Q}_{w,DHW}\cdot dt}{60} \quad \text{(eq. 7)}$$

where the differential dt refers to the 1 – minute intervals while the value 60 is used for converting minutes to hours.

3.3. Uncertainty analysis

The propagation of sensors accuracies through the calculated properties is identified according to (Meramveliotakis et al., 2022) with the systematic error ε of a given calculated value y estimated by Eq. 8.

$$\varepsilon_y=\sqrt{\sum_i \left(\frac{\partial y}{\partial x_i}\right)^2 \varepsilon_{x_i}^2} \quad \text{(eq. 8)}$$

where $\varepsilon_{\chi i}$ is the uncertainty of the independent variables and $\frac{\partial y}{\partial x_i}$ the partial derivative of the y function with respect to every independent variable x_i.

4. Results and Discussion

4.1. Ambient conditions on reference days

According to the previous analysis, the experiments took place at 30-31 of July 2022 in Athens. The Day 1 refers to the "M" DHW profile while the Day 2 to the "L" one. The ambient conditions of these days are depicted in Fig 4 with an average ambient temperature of 29.24 during Day 2.

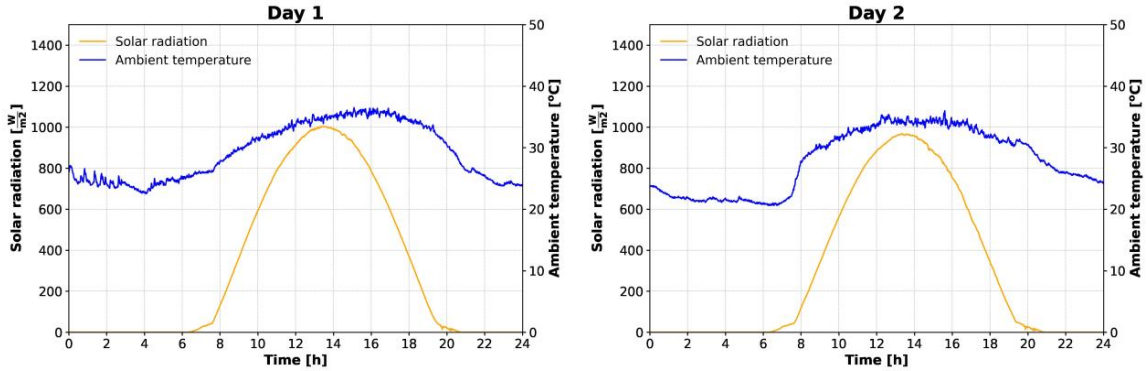

Fig. 4: Ambient temperature and solar radiation during the two days

The average daylight was about 14 hours and 9 minutes of clear sky for both days. As a result, the incident radiation on the surface of the collectors has very similar values for both days with a peak of about 1000 W/m^2 at 13:20 local time which coincides with the solar noon hour. It is obvious that due to the high ambient temperature and the plenty of solar irradiation the heat pump is expected to operate for a very short period of time during the day and especially when DHW is needed and there is no availability of solar irradiation (for example early in the morning or at night).

4.2. System performance

4.2.1. PVT performance

The performance of the PVT collectors is examined next. The heat and electricity production in accordance to the inlet and outlet brine temperatures of the collectors is shown in Fig. 5, as well as the thermal and electrical efficiency.

The control of the pump in the solar circuit was set to operate when the inlet temperature of PVT collectors is above 20 ^oC and the temperature difference between inlet and outlet brine is greater than 1 K. For that reason, at about 09:00 am, some fluctuations of heat production are observed, due to the fact that a period of time is needed in order to balance the transient phenomena and to obtain constant positive temperature difference between inlet and outlet flows at the collectors. The duration of heat production from PVTs during the day was about 7.5 hours for both days starting at about 9:20 and until 16:50. Also, heat production and thermal efficiency curves have the same peaks at almost identical times in both days, when the DHW tank is discharged due to taping, reducing the tank temperature, which is beneficial for the PVT efficiency. The maximum thermal performance of the PVTs occurs at noon between 12:00 and 14:00 with an average maximum production of 1.43±0.09 kW.

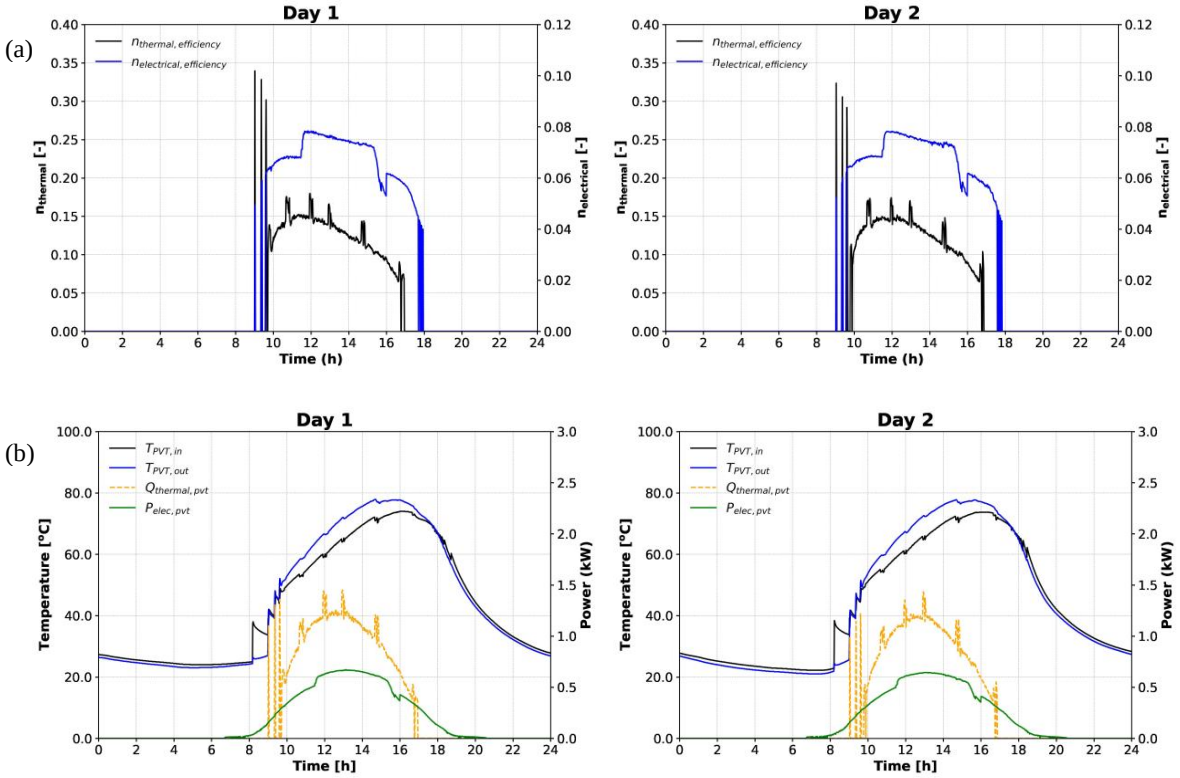

Fig. 5: PVT collectors performance indicators. (a) Thermal end electrical efficiency; (b) inlet and outlet temperature, heat and electricity production

Focusing on the electrical part of PVT collectors, the PV cells produce electricity for about 11 hours and 18 minutes from 7:54 to 19:12 on both days. The electricity generation follows an almost smooth curve with some fluctuations depending on the sun availability and brine temperature. From Fig. 5 is shown that the peak production occurs from 12:00 to 14:00 showing a maximum performance of 0.66±0.03 kW on average, due to the higher IAM values depending on the incidence angle of solar radiation on the tilted collectors. This effect is caused by movement of the shade created by the aluminum frame on both the reflector trough and the reflector underside as the sun moves from horizon to zenith affecting the energy generation of the PV cells on the lower side (Gomes et al., 2014).

The main performance indicators of PVT collectors are shown in Tab. 3 indicating an average daily efficiency for the electricity production of 6.97±0.04% and for heat of 12.69±0.03%. Concerning the production over the whole day, the heat production was about 6.77±0.09 kWh and the electrical production 4.31±0.14 kWh.

Tab. 3: Performance indicators of the PVT collectors

Performance indicator	Units	Day 1	Day 2
Peak heat production	kW	1.44	1.43
Daily thermal energy	kWh	7.00	6.54
Peak thermal efficiency	%	33.95	32.35
Average thermal efficiency	%	12.76	12.63
Peak electrical production	kW	0.67	0.644
Daily electric energy	kWh	4.40	4.23
Peak electrical efficiency	%	7.83	7.82
Average electrical efficiency	%	6.96	6.99

4.2.2. DHW production

The daily variation of the properties relevant to the DHW tank is shown in Fig. 6. The average inlet temperature of the tapping water is about 30 ºC (significantly high due to the summer days) with some fluctuations at the time when the DHW valve opens and the standing water inside the piping starts to circulate. The average DHW outlet temperature is about 50 ºC and the water tank is 60 ºC in both days. From Fig. 6 it is observed that the outlet water temperature reaches almost the tank temperature with a small margin of 2-3 ºC especially from 14:00 to 18:00 when the tank temperature is high due to the charging from the collectors.

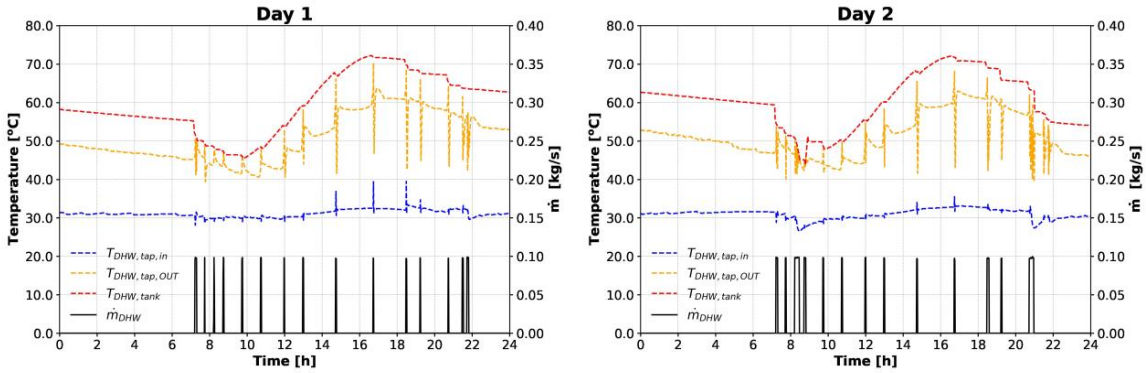

Fig. 6: Water temperatures and mass flow rate of the DHW tank during both days

The water temperatures and DHW production are shown in Tab. 4 for both days, with the measured DHW consumption being 5.73±0.38 kWh (22% higher in Day 1 with "M" profile) and 9.62±0.38 kWh (3% higher in Day 2 with "L" profile) compared to the reference values of the standard. This discrepancy depends mostly on the variation of the water inlet temperature along with the time period which is required for the electronic valve to fully open (about 0.5 min) and to fully close (about 1 min) during the operation.

Tab. 4: Main indicators of domestic hot water production in both days

DHW production	Units	Day 1	Day 2
Daily DHW production	kWh	5.73	9.62
DHW thermal energy (reference)	kWh	4.68	9.34
Total time of DHW valve opening	min	31.00	62.00
Average DHW inlet temperature	ºC	31.14	31.01
Average DHW outlet temperature	ºC	50.79	51.26
Average DHW tank temperature	ºC	59.68	60.30

4.2.3. Heat pump operation

The DHW tank temperature is kept above the threshold of 45 ºC during most of testing period, due to the high ambient temperatures, the high temperature of tapping water (about 30 ºC) and the plenty of solar irradiation. This leads to no or very little operation of the heat pump. According to Fig. 7, when the "M" profile is considered, the heat pump does not operate during the day as the DHW tank temperature is always above the setpoint. Otherwise, during the second day the energy demand is higher and the heat pump needs to operate to increase the tank temperature to 50 ºC which is the upper margin of the on-off control (Fig. 6). As a result, the heat pump operates for 10 minutes during the whole day and specifically from 08:47 until 08:57 to provide the required thermal energy to the system.

The average electrical consumption of the compressor is about 3.80±0.19 kW (0.511±0.07 kWh during the day) operating at 50 Hz when the tank temperature is much lower than the set-point (electrical consumption about 4.5±0.22 kW) with the inverter adjusting its speed and gradually reduce it to 35 Hz (electrical consumption about 3.4±0.17 kW) when the tank temperature reaches the setpoint with 1 K margin. Additionally, the capacity of the heat pump reaches high values resulting to an average of 17.43±0.69 kW, due to the high outdoor temperature of about 30 ºC, charging the tank with 2.17±0.11 kWh during this period. The system and compressor COP have an average value

of 3.42±0.21 and 3.85±0.21 respectively (main difference is the power of the air fans, about 0.43 kW) while the PVT daily electrical production is 6 times higher than the electricity demand. Tab. 5 shows the performance indicators of the heat pump only during the second day with the "L" profile.

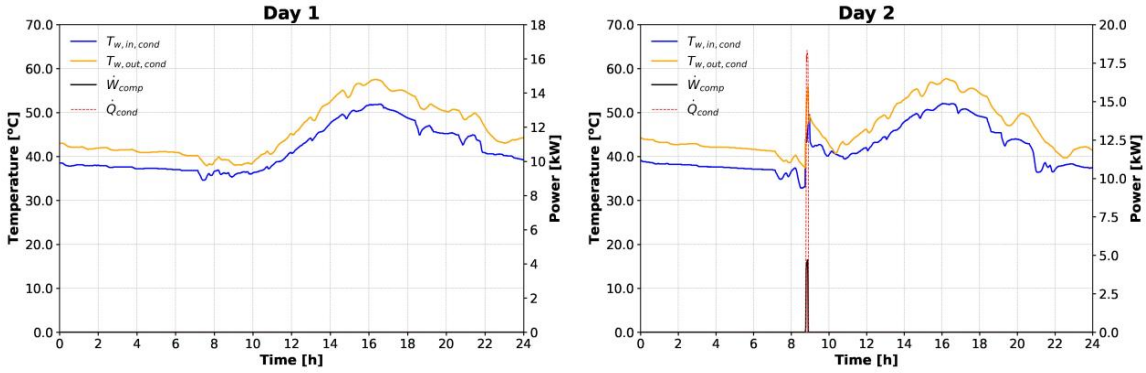

Fig 7: Heat pump operation during the days of the measurements

Tab. 5: Performance indicators of the heat pump during the second day

Heat pump performance	Units	Day 2
Average compressor COP	-	3.85
Average system COP	-	3.42
Average heating capacity	kW	17.43
Daily heat production	kWh	2.17
Daily electricity consumption	kWh	0.58
Daily compressor electricity consumption	kWh	0.51

5. Conclusions

A renewable energy system combining a dual source heat pump and four PVT concentrating stationary collectors is examined experimentally for domestic hot water production. The tests took place in two consecutive summer days in Athens, Greece, with two different tapping water profiles (one for each day) with a calculated thermal energy draw-off profile of 4.68 kWh for the first day ("M" profile) and 9.34 kWh for the second one ("L" profile) according to the EU standard.

The experimental procedure revealed that the PVT collectors provided an average thermal and electrical capacity of 6.8 kWh and 4.3 kWh respectively being similar for both days, resulting to 12.7% thermal and 7% electrical efficiency. Both thermal and electrical production have their peak during noon from 12:00 to 14:00 due to higher IAM values and the increased solar irradiation availability. Owing to the summer ambient conditions and the high temperature of the tapping water (about 30 ^{o}C) the PVT heat production is capable to keep the temperature of the DHW tank above 45 ^{o}C for the whole day with the "M" profile, while with the "L" profile requires a very little use of the heat pump in order to maintain the water temperature in the tank within the desired levels. Concerning the performance of the heat pump, it is operated only on air source heating mode for about 10 minutes during the second day. The average system and compressor COP was 3.42 and 3.85 respectively providing 2.17 kWh of thermal energy to the DHW tank. Because of the limited (day with "L" profile) or no (day with "M" profile) use of the heat pump over the day, the daily produced electricity of the PVT collectors is about 6 times higher than the electricity consumption of the heat pump, indicating that the system can provide domestic hot water and electricity exclusively derived from renewables during the summer days. However, this is expected to greatly decrease during intermediate seasons and especially winter.

In the next steps, the system will be examined experimentally for the whole year introducing not only different

tapping profiles but also different configurations of the heat pump and PVT collectors, also under SAHP operation, taking advantage of the flexibility of the pilot system. After that, a complete evaluation of the system can be accomplished, examining the performance of every component with special attention to the heat pump operation under both water and air source operation. In parallel, optimization control algorithms will be integrated to combiner the different functionalities of the system and thus minimize the net electricity consumption by increasing at the same time as much as possible the exploitation of renewable energy sources.

6. Acknowledgments

This work has been performed within the RES4BUILD project (Renewables for clean energy buildings in a future power system) – Horizon 2020 program, Grant Agreement no. 814865.

7. References

Bertoldi, P., Diluiso, F., Castellazzi, L., Labanca, N., Serrenho, T., 2018. Energy consumption and energy efficiency trends in the EU-28 2000-2015. JRC Report, European Commission.

Buker, M.S., Riffat, S.B., 2016. Solar assisted heat pump systems for low temperature water heating applications: A systematic review. Renewable and Sustainable Energy Reviews 55, 399–413. https://doi.org/10.1016/J.RSER.2015.10.157

Directive 2009/125/EC of the European Parliament and of the Council with regard to ecodesign requirements for water heaters and hot water storage tanks, EU Regul. No 814/2013 2 August 2013 – Available at: https://eur-lex.europa.eu/eli/reg/2013/814/2017-01-09 (Accessed at: 25 August 2022)

Galindo Marina, Roger-Lacan Cyril, Gährs Uwe, Aumaitre Vincent, 2016. Efficient district heating and cooling markets in the EU: Case studies analysis, replicable key success factors and potential policy implications. Publications Office of the European Union, Luxembourg (Luxembourg). https://doi.org/10.2760/371045

Gomes, J., Diwan, L., Bernardo, R., Karlsson, B., 2014. Minimizing the Impact of Shading at Oblique Solar Angles in a Fully Enclosed Asymmetric Concentrating PVT Collector. Energy Procedia 57, 2176–2185. https://doi.org/10.1016/J.EGYPRO.2014.10.184

Guo, X., Goumba, A.P., 2018. Air source heat pump for domestic hot water supply: Performance comparison between individual and building scale installations. Energy 164, 794–802. https://doi.org/10.1016/J.ENERGY.2018.09.065

Ju, F., Fan, X., Chen, Y., Ouyang, H., Kuang, A., Ma, S., Wang, F., 2018. Experiment and simulation study on performances of heat pump water heater using blend of R744/R290. Energy Build 169, 148–156. https://doi.org/10.1016/J.ENBUILD.2018.03.063

Kosmadakis, G., Arpagaus, C., Neofytou, P., Bertsch, S., 2020. Techno-economic analysis of high-temperature heat pumps with low-global warming potential refrigerants for upgrading waste heat up to 150° C. Energy Convers Manag 226, 113488. https://doi.org/10.1016/j.enconman.2020.113488

Kwon, C., Kim, Mo Se, Choi, Y., Kim, Min Soo, 2017. Performance evaluation of a vapor injection heat pump system for electric vehicles. International Journal of Refrigeration 74, 138–150. https://doi.org/10.1016/J.IJREFRIG.2016.10.004

Lämmle, M., Oliva, A., Hermann, M., Kramer, K., Kramer, W., 2017. PVT collector technologies in solar thermal systems: A systematic assessment of electrical and thermal yields with the novel characteristic temperature approach. Solar Energy 155, 867–879. https://doi.org/10.1016/J.SOLENER.2017.07.015

Li, J., Fan, Y., Zhao, X., Bai, X., Zhou, J., Badiei, A., Myers, S., Ma, X., 2022. Design and analysis of a novel dual source vapor injection heat pump using exhaust and ambient air. Energy and Built Environment 3, 95–104. https://doi.org/10.1016/J.ENBENV.2020.11.004

Long, J., Xia, K., Zhong, H., Lu, H., A, Y., 2021. Study on energy-saving operation of a combined heating system of solar hot water and air source heat pump. Energy Convers Manag 229, 113624.

https://doi.org/10.1016/J.ENCONMAN.2020.113624

Meramveliotakis, G., Kosmadakis, G., Karellas, S., 2022. Identifying the performance and losses of a scroll compressor with vapour injection and R1234ze(E). Open Research Europe 2, 49. https://doi.org/10.12688/openreseurope.14658.2

Meramveliotakis, G., Kosmadakis, G., Karellas, S., 2022. Methods based on a semi-empirical model for simulating scroll compressors with HFC and HFO refrigerants. Open Research Europe 1, 148. https://doi.org/10.12688/openreseurope.14313.3

Nuntaphan, A., Chansena, C., Kiatsiriroat, T., 2009. Performance analysis of solar water heater combined with heat pump using refrigerant mixture. Appl Energy 86, 748–756. https://doi.org/10.1016/J.APENERGY.2008.05.014

Panaras, G., Mathioulakis, E., Belessiotis, V., 2014. A method for the dynamic testing and evaluation of the performance of combined solar thermal heat pump hot water systems. Appl Energy 114, 124–134. https://doi.org/10.1016/J.APENERGY.2013.09.039

Panaras, G., Mathioulakis, E., Belessiotis, V., 2013. Investigation of the performance of a combined solar thermal heat pump hot water system. Solar Energy 93, 169–182. https://doi.org/10.1016/J.SOLENER.2013.03.027

Pezzutto, S., Croce, S., Zambotti, S., Kranzl, L., Novelli, A., Zambelli, P., 2019. Assessment of the Space Heating and Domestic Hot Water Market in Europe—Open Data and Results. Energies (Basel) 12, 1760. https://doi.org/10.3390/en12091760

Pilou, M., Kosmadakis, G., Meramveliotakis, G., Krikas, A., 2022. Towards a 100% renewable energy share for heating and cooling in office buildings with solar and geothermal energy. Solar Energy Advances 100020. https://doi.org/10.1016/J.SEJA.2022.100020

Pilou, M., Kosmadakis, G., Meramveliotakis, G., Krikas, A., 2021. Renewable Energy Based Systems with Heat Pumps for Supplying Heating and Cooling in Residential Buildings. https://doi.org/10.5281/ZENODO.5291855

Sterling, S.J., Collins, M.R., 2012. Feasibility analysis of an indirect heat pump assisted solar domestic hot water system. Appl Energy 93, 11–17. https://doi.org/10.1016/J.APENERGY.2011.05.050

Sun, X., Dai, Y., Novakovic, V., Wu, J., Wang, R., 2015. Performance Comparison of Direct Expansion Solar-assisted Heat Pump and Conventional Air Source Heat Pump for Domestic Hot Water. Energy Procedia 70, 394–401. https://doi.org/10.1016/J.EGYPRO.2015.02.140

Tello-Oquendo, F.M., Navarro-Peris, E., Barceló-Ruescas, F., Gonzálvez-Maciá, J., 2019. Semi-empirical model of scroll compressors and its extension to describe vapor-injection compressors. Model description and experimental validation. International Journal of Refrigeration 106, 308–326. https://doi.org/10.1016/j.ijrefrig.2019.06.031

Tian, Z., Zhang, S., Deng, J., Fan, J., Huang, J., Kong, W., Perers, B., Furbo, S., 2019. Large-scale solar district heating plants in Danish smart thermal grid: Developments and recent trends. Energy Convers Manag 189, 67–80. https://doi.org/https://doi.org/10.1016/j.enconman.2019.03.071

Vaishak, S., Bhale, P. v., 2019. Photovoltaic/thermal-solar assisted heat pump system: Current status and future prospects. Solar Energy 189, 268–284. https://doi.org/10.1016/J.SOLENER.2019.07.051

Wang, W., Li, Y., 2019. Intermediate pressure optimization for two-stage air-source heat pump with flash tank cycle vapor injection via extremum seeking. Appl Energy 238, 612–626. https://doi.org/10.1016/J.APENERGY.2019.01.083

Zhou, X., Tian, S., An, J., Yan, D., Zhang, L., Yang, J., 2022. Modeling occupant behavior's influence on the energy efficiency of solar domestic hot water systems. Appl Energy 309, 118503. https://doi.org/10.1016/J.APENERGY.2021.118503